Biochimica et Biophysica Acta 1827 (2013) 233–238

Contents lists available at SciVerse ScienceDirect

Biochimica et Biophysica Acta

journal homepage: www.elsevier.com/locate/bbabio

Electrochemical behaviour of bacterial nitric oxide reductase—Evidence of low redox potential non-heme Fe_B gives new perspectives on the catalytic mechanism

Cristina M. Cordas *[,1], Américo G. Duarte [1,2], José J.G. Moura, Isabel Moura

Requimte, Centro de Química Fina e Biotecnologia, Departamento de Química, Faculdade de Ciências e Tecnologia, Universidade Nova de Lisboa, Quinta da Torre, 2829-516 Monte de Caparica, Portugal

ARTICLE INFO

Article history:
Received 24 May 2012
Received in revised form 26 October 2012
Accepted 31 October 2012
Available online 7 November 2012

Keywords:
Denitrification
Electrochemistry
Enzymatic catalysis
Metalloenzyme
Nitric oxide reductase

ABSTRACT

Nitric oxide reductase (NOR) is a membrane bound enzyme involved in the metabolic denitrification pathway, reducing nitric oxide (NO) to nitrous oxide (N_2O), subsequently promoting the formation of the N–N bond. Three types of bacterial NOR are known, namely cNOR, qNOR and qCuNOR, that differ on the physiological electron donor. cNOR has been purified as a two subunit complex, the NorC, anchored to the cytoplasmic membrane, with a low-spin heme *c*, and the NorB subunit showing high structural homology with the HCuO subunit I, comprising a bis-histidine low-spin heme *b* and a binuclear iron centre. The binuclear iron centre is the catalytic site and it is formed by a heme b_3 coupled to a non-heme iron (Fe_B) through a μ-oxo bridge. The catalytic mechanism is still under discussion and three hypotheses have been proposed: the *trans*-mechanism, the *cis*-Fe_B and the *cis*-heme b_3 mechanisms. In the present work, the *Pseudomonas nautica* cNOR electrochemical behaviour was studied by cyclic voltammetry (CV), using a pyrolytic graphite electrode modified with the immobilised protein. The protein redox centres were observed and the formal redox potentials were determined. The binuclear iron centre presents the lowest redox potential value, and discrimination between the heme b_3 and Fe_B redox processes was attained. Also, the number of electrons involved and correspondent surface electronic transfer rate constants were estimated. The pH dependence of the observed redox processes was determined and some new insights on the NOR catalytic mechanism are discussed.

1. Introduction

Nitric oxide reductase (NOR) is an integral membrane enzyme involved in the metabolic denitrification pathway, reducing nitric oxide (NO) to nitrous oxide (N_2O), subsequently promoting the formation of the N–N bond [1]. This class of enzymes belongs to the heme copper oxidase (HCuO) superfamily presenting additional oxidoreductase activity, and, although non-electrogenic and not pumping protons across the membrane, these proteins take the necessary protons from the periplasmic site of the membrane for the NO or O_2 reduction [2]. Three types of bacterial NOR are known, namely cNOR, qNOR and qCuNOR, that differ on the physiological electron donor, such as soluble cytochromes, azurin or quinol, the number of subunits and the electronic transfer centre composition, from heme co-factors to binuclear Cu centres [1,3,4]. cNOR has been isolated from several denitrifying organisms, such as *Paracoccus denitrificans* [5,6], *Halomonas halodenitrificans* [7,8], *Pseudomonas nautica* [9], *Pseudomonas stutzeri* [10,11] and *Pseudomonas aeruginosa* [12]. It has been purified as a two subunit complex, the NorC, of 17 kDa, proposed to be anchored to the cytoplasmic membrane, with a low-spin heme *c*, and the NorB subunit, of 54 kDa, which shows a high structural homology with the HCuO subunit I, comprising a bis-histidine low-spin heme *b* and a binuclear iron centre. The binuclear iron centre is the catalytic site and it was shown to be formed by a heme b_3 coupled to a non-heme iron (Fe_B) through a μ-oxo bridge [13]. A recent spectroscopic study revealed that heme b_3 is low-spin in both oxidised and reduced states on cNOR from *P. nautica* [9]. Moreover, the first crystal structure of cNOR was obtained in the presence of specific fragment antibodies, at 2.7 Å resolution [14]. The published data confirmed the previously predicted metal co-factors, as well as the low-spin configuration of the catalytic heme site. A schematic representation of the cNOR co-factors is presented in Fig. 1.

The catalytic mechanism is still under discussion and three hypotheses have been proposed: the *trans*-mechanism [12,15,16], the *cis*-Fe_B [9,17–20] and the *cis*-heme b_3 mechanism [21,22]. All proposed mechanisms agree in the possible formation of a hyponitrite anion as one of the transient species after the N–N bond formation between the two NO molecules [1,23].

In the literature, redox potentials of *P. denitrificans* NOR obtained by potentiometric titrations show that low-spin heme *c*, heme *b* and Fe_B potentials are in the range of 300–350 mV and 60 mV for the catalytic heme b_3. Based on this information, a three electron reduced form of the enzyme, was initially proposed as the active form [24].

* Corresponding author. Tel.: +351 212 948 316.
E-mail address: cristina.cordas@fct.unl.pt (C.M. Cordas).
[1] Both authors contributed equally for this scientific work.
[2] Current address: Instituto de Tecnologia Química e Biologica/Universidade Nova de Lisboa, Av. da República, Estação Agronómica Nacional, 2780-157 Oeiras, Portugal.

0005-2728/$ – see front matter © 2012 Elsevier B.V. All rights reserved.
http://dx.doi.org/10.1016/j.bbabio.2012.10.018

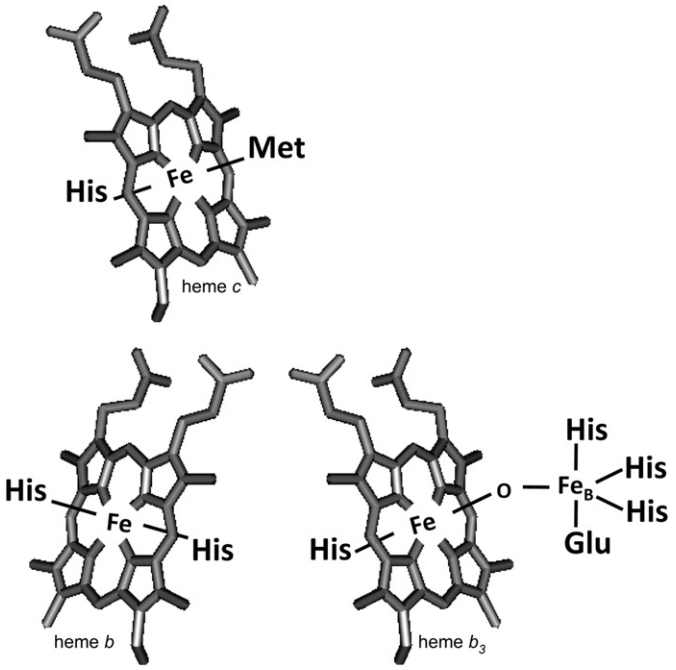

Fig. 1. Schematic representation of the cNOR metal co-factors.

Later, kinetic and spectroscopic studies indicated that the four electron reduced NOR is the active form of the enzyme [9], suggesting a revision of the iron sites' redox potential and catalytic mechanism. Recently, *P. nautica* NOR midpoint potentials of the low-spin electron transfer hemes and the catalytic heme b_3 were determined with values respectively of +215 mV and −38 mV [9]. Direct electrochemical measurements allowed the observation of the redox behaviour of NOR isolated from the same organism, revealing a well defined redox process, indexed to the binuclear iron centre, showing a lower midpoint potential than previously reported, namely −126 mV [25]. Using a structural and functional NOR model, constructed starting from the sperm whale myoglobin, a redox potential for the high-spin heme *b* of −158 mV was determined, being this value shifted to −46 mV when magnetic coupling is established between the heme and non-heme iron [26].

Spectroelectrochemistry studies proposed the catalytic binuclear iron centre to be isopotential, with a redox potential of 80 mV below the values determined for the electron transfer hemes *b* and *c*. Experiments conducted under CO atmosphere suggested that upon substrate binding the binuclear redox potential will increase its value and a structural conformation variation would be expected [27].

In the present work, the *P. nautica* NOR electrochemical behaviour was studied by cyclic voltammetry (CV) using a pyrolytic graphite electrode modified with the immobilised protein. The formal potentials of the observed redox processes, number of electrons involved and correspondent surface electronic transfer rate constants were estimated. Also, the pH dependence of the redox processes was determined and some new insights on the NOR catalytic mechanism are discussed.

2. Materials and methods

2.1. Protein purification

Nitric oxide reductase was purified from membrane extracts of *P. nautica* 617, grown anaerobically in the presence of nitrate. The purity of the protein fraction was estimated by UV–visible spectra and SDS-PAGE. Iron content was obtained by heme quantification and total iron content determined by ICP as described elsewhere [9].

2.2. Protein immobilisation

Protein immobilisation on the working electrode, a pyrolytic graphite disk electrode (Ø = 0.4 cm), was accomplished by adsorption using solvent casting technique. Each assay was performed using pure protein sample (7 μL of 265 μM) equilibrated in 100 mM potassium phosphate buffer pH 7.0, 0.02% (v/v) n-Dodecyl β-D-maltoside, and 0.01% (S)-(−)-phenylethanol. Control experiments were performed in the absence of the immobilised enzyme. Prior to use, the electrode graphite was treated through immersion in concentrated nitric acid solution, rinsed in water, and polished with 5.0, 1.0 and 0.3 μm alumina, after that it was rinsed with Millipore water and submitted to an ultra-sonic bath for 1 min and again thoroughly rinsed with Millipore water.

2.3. Electrochemical mesurements

Cyclic voltammetry (CV) experiments were performed using a μAUTOLAB potentiostat, in one compartment electrochemical cell and three electrode configuration. Pyrolytic graphite disk electrode was used as working electrode. A platinum wire and a saturated calomel electrode (SCE) were the counter and reference electrodes, respectively. The supporting electrolyte solution was a mixture of sodium citrate/MES/HEPES/AMPSO buffers, of 20 mM for each component, buffered from pH 2.1 to 9.7 and all the reagents were of analytical grade. Data acquisition was performed using the GPES (Eco Chimie) software. All electrochemical experiments were performed at room temperature, in an anaerobic chamber (MBRAUN), where O_2 concentration was 0.1 ppm. CV assays were performed at different scan rates (from 5 mV to 5 V s^{-1}).

2.4. Measurements under catalytic conditions

Electrochemical measurements in the presence of substrates were conducted analogously to that described in the previous section. O_2 and NO additions were made from water solutions saturated with the dissolved gas. O_2 dissolved gas solution was made by direct bubbling from a 100% oxygen bottle (Air Liquide). NO dissolved gas solution was achieved by bubbling the 5% NO/95% He mixture in 5 M KOH solution and through non buffered water at pH 3, to remove possible NOx formation, before water bubbling.

3. Results and discussion

3.1. Electrochemical characterization

The direct electrochemical response of the immobilised NOR was attained showing the presence of four different redox couples, designated I to IV from the more negative to the more positive potential values (Fig. 2). Another cathodic peak is also visible close to 300 mV but this process is present on the control assays and it should result from the reduction of surface oxides on the graphite electrode. The NOR midpoint potentials have been determined for processes I, II, III and IV, at pH 7.6, and the corresponding values are -369 ± 14 mV, -162 ± 9 mV, 43 ± 12 mV and 208 ± 17 mV, respectively. Process II was already described in the literature, and it has been observed at midpoint potential of -126 ± 13 mV at pH 7.6, and attributed to the binuclear centre [25]. From the charge, associated to the anodic or the cathodic current peaks of this well-defined process II, the electrode surface coverage was estimated as $2.37 \pm 0.27 \times 10^{-11}$ mol/cm^2, corresponding to a multilayer coating. All the observed redox pair current intensities are scan rate dependent, as expected for surface confined processes (see data in Supplementary Information). From the scan rate dependence, and using Laviron's formulation [28], it was possible to estimate the surface electron transfer rate constant, k_s, for each process. The k_s constant is an indicative parameter of how facilitated is the communication between the enzyme and the electrode surface and it can be seen as a measure

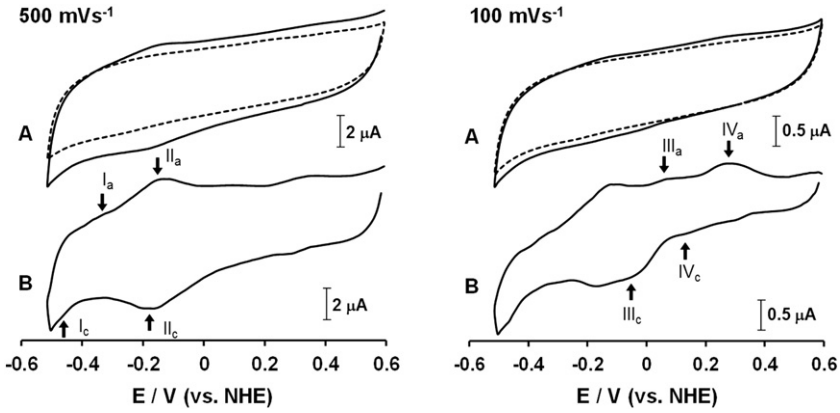

Fig. 2. Cyclic voltammograms of immobilised *P. nautica* NOR at different scan rates (100 and 500 mV s^{-1}). A) black line—CV with the immobilised enzyme and dashed line—control experiment, without the enzyme. B) Correspondent subtraction of the upper voltammograms. Experiments were conducted as described on experimental section at pH = 7.6.

of the relative electrochemical efficiency of the immobilized protein [29]. From the results, summarised in Table 1, it can be observed that processes I and II present higher k_s than processes III and IV, in agreement with the voltammetric behaviour variation with the scan rate. In fact, processes I and II are better defined at higher scan rates and III and IV can be better observed at lower scan rates (typically, higher and lower than 500 mV s^{-1}, for I and II, and III and IV, respectively—see Fig. 2). For all the processes, the anodic and cathodic current ratio is approximately one and the estimated formal redox potentials are independent of the scan rate. From the value of the processes' peak width at half current height ($\Delta Ep_{1/2}$) an attempt to estimate the number of electrons involved was made. The results for the four observed processes indicate that in each centre one electron is involved, namely, 1.30 ± 0.43, 0.52 ± 0.16, 0.99 ± 0.38 and 1.35 ± 0.50, respectively for processes I to IV. The number of electrons obtained for the processes is, in general, shifted from the expected theoretical value, in particular, for process II, as an effect of the broadening of the peaks. This effect has been observed in other systems [30–33] and interpreted as due to dispersion of formal potentials or rate constants, arising from different local environments and interactions as a consequence of a dense protein film. In fact, considering the electrode area, the calculated coverage and the NOR dimensions, it is possible to estimate approximately 2.5 layers of immobilised NOR. This dense coverage is expected to influence the electron transfer and seems in agreement with the observed electrochemical behaviour. The estimated number of electrons seems consistent with the proposed mechanism for NOR implying four electron reduced species as the enzyme active form [9] and sequential electron transfer, since in the catalytic cycle the first two demanded electrons are obtained from the ferrous catalytic di-iron centre and the subsequent required electrons are delivered to the catalytic iron centres from the heme *c* and *b* electron transfer centres. Studies have shown that the four electron reduced NOR form is essential for the catalytic cycle initiation and that the intramolecular electron transfer between the low-spin heme *b* and the catalytic heme b_3 is substrate dependent [34]. Additionally, our own kinetic data of *P. nautica* NOR show that this internal electron transfer is crucial to explain the different kinetic profiles achieved with the different substrates (manuscript in preparation). In the literature [9,24,27], the two higher potential redox processes are attributed to hemes *b* and *c*, the enzymes' electronic transfer redox centres. In our data, two processes (III and IV) are also visible at high potentials (in the near range of 40 to 200 mV), and so, by analogy with that reported in the literature, processes III and IV (Fig. 2), with the higher potential values, should be assigned to heme *b* and heme *c*, respectively. The full spectroscopic characterization of the enzyme, has shown that the low-spin electron transfer hemes are reduced after sodium ascorbate addition [9]. Therefore, attributing the higher redox process to heme *c* is expected, since this domain is exposed to the periplasmatic site of the membrane and responsible for docking with the physiologic electron donor (cyt. c_{552}) [9,35,36], enhancing the electron transfer towards the catalytic site.

Table 1
P. nautica NOR co-factor midpoint redox potentials, surface electronic transfer rate constant and number of electrons.

Process	Metal centre	E (mV)	k_s (s^{-1})[a]	n[b]
I	Fe_B	-369 ± 14	73 ± 10	1.30 ± 0.43
II	Heme b_3	-162 ± 9	129 ± 26	0.52 ± 0.16
III	Heme *b*	43 ± 12	6.4 ± 2	0.99 ± 0.38
IV	Heme *c*	208 ± 012	17.4 ± 5	1.35 ± 0.50

[a] k_s values for scan rate 5 V s^{-1} for non-heme Fe_B and heme b_3 and 500 mV s^{-1} for hemes *b* and *c*.
[b] n, number of electrons, estimated from $\Delta Ep_{1/2}$ at 20 °C, pH 7.6.

3.2. NO and O_2 reduction

Previously, NOR was shown to have catalytic activity towards O_2 reduction, in addition to NO reduction to N_2O [25,37]. In Fig. 3, cyclic voltammograms obtained in the presence and absence of the enzyme substrates are displayed and one can observe the catalytic wave, a consequence of O_2 reduction, which starts to develop approximately at 0 mV. The present data confirms the previous results [25] and show that the electrocatalytic response due to the enzyme reduction of O_2, is detected at a potential value close to the process II midpoint potential around −140 mV where the maximum of the reduction current peak at 50 mV s^{-1} is observed.

On cytochrome *c* oxidases (CcO), presenting O_2 reduction activity, O_2 binds to the binuclear centre probably to the catalytic heme [2]. Electrochemistry studies on C*c*O models immobilised on self-assembled monolayers (SAM), where the electron transfer rate towards the metal centres was tuned by changing the SAM length and degree of conjugation, have shown that O_2 binds to the heme a_3, although the presence of Cu_B is crucial for the reduction of partial reduced oxygen species [38]. By analogy with C*c*O family, its function and structural similarity, regarding the O_2 reduction activity [39], it is expected that in NOR the O_2 will bind to the binuclear centre and probably to the catalytic heme b_3 [2]. Therefore, process II that was previously attributed to the catalytic binuclear centre [25], is now proposed to be due to the catalytic heme b_3 redox centre.

Our data show the presence of another redox process (named I), observed at more negative potentials (midpoint potential ca. −370 mV). This was attributed to the non-heme Fe_B. Mössbauer spectroscopy data showed that the Fe_B centre is not fully reduced by sodium dithionite [9] which is an indication of its negative redox potential. Also, the presence of ligands with electron donating character, such as the μ-oxo/hydroxo bridge between the non-heme Fe_B and heme b_3, has been reported to

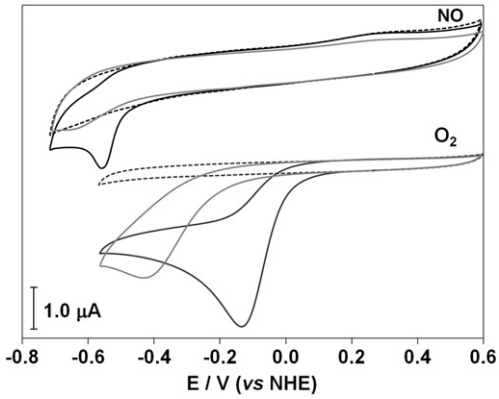

Fig. 3. Cyclic voltammograms of NO and O_2 reduction obtained with the immobilised enzyme modified electrode, in the presence of substrate (black line) and in the absence of substrate (dashed line); control assays with the substrate without adsorbed enzyme (grey line); $v = 50$ mV s^{-1}; $[NO] = 20$ μM and $[O_2] = 56$ μM. The voltammograms obtained in the presence of O_2 were multiplied by 0.4 to make comparison easier.

influence the centre's formal potentials by lowering its value in several inorganic and biological relevant systems [40–42]. From the literature, it is also known that the distance between the two catalytic irons (3.9 Å [14]) does not allow the binding of two NO molecules to both metals at the same time, suggesting that Fe_B is also reduced, breaking the μ-oxo/hydroxo bridge and lengthening the distance between the two irons [36] inducing conformational changes that may also influence the potential of Fe_B [43]. Additionally, the current response associated to the NO reduction is observed approximately at −560 mV and the catalytic peak starts to develop around −450 mV, close to process I cathodic peak potential, which is in agreement with conformational changes associated with the centre reduction. These data agree with redox potentials determined for the first inorganic model compound that mimics the NOR non-heme Fe_B site [44]. The summary of the redox processes' assignment to NOR four redox centres is shown in Table 1.

Some discussions concerning the enzyme's native state are frequent. From our results it is possible to infer that the adsorbed NOR retains its activity similarly to the native protein. First observation is the development of catalytic currents in the presence of the NOR substrate, which increase upon the NO concentration increment. Additionally, kinetic experiments, performed with the adsorbed *P. nautica* NOR using a rotative disk electrode (see Supplementary Information) and parallel assays with the protein in solution, using cyt c_{552} as electron donor, in the presence of NO (manuscript in preparation), allowed one to calculate the k_{cat} values. For the immobilised NOR the value is 11.6 s^{-1}, which is lower than the one found with the enzyme in solution (30.4 s^{-1}). The activity differences between immobilised versus in solution enzyme are not uncommon and there are previous reported examples with other biological systems [45,46]. Also, the pH dependence study of the different redox centres and the determined pK values are in agreement to previous work [25] (see following section and Table 2). So, from the facts and, although with some activity loss, the statement that in our experimental conditions NOR retains its properties is reasonable. However, it should be noticed that the results achieved with immobilized NOR, although giving indications on the enzymes' behaviour, should not be taken to perform direct comparisons to the native NOR in physiological conditions.

The electrochemical behaviour of NOR in the presence of NO was also observed (see Fig. 4), confirming previous results [25]. Assays performed varying the scan rate from 5 mV s^{-1} up to 5 V s^{-1}, have shown that the midpoint potential value of process II, attributed to heme b_3, does not shift in the presence of NO, as displayed in Fig. 4. The maximum shift is around 10 mV, observed at the scan rate of 5 V s^{-1}, which is within the determined experimental error (see Table 1). Considering the proposed catalytic mechanisms for NO, namely the *trans* and the *cis*-heme b_3 mechanisms, a shift on the heme b_3 redox potential upon the catalytic cycle due to NO binding should be expected, in agreement with results obtained with CO, where the binding to heme b_3 induced a shift towards more positive potentials [27]. Our data show no shift on heme b_3 redox potential and, therefore, it seems to point to a mechanism in which the two NO molecules bind to Fe_B, supporting the so-called *cis*-Fe_B mechanism [9,17–20]. Further experiments are needed to confirm this assumption. This hypothesis is consistent with the heme b_3 role of maintaining the oxo/hydroxo bridge coordination, supplying the reductive equivalents for the catalytic reaction and abstracting the O atom, triggering the product release [9].

3.3. pH dependence

The pH dependence of the four observed redox processes' potential was evaluated. From the data it was possible to confirm that all the centres' formal potential values change with the pH (Fig. 5). The best data fit of the obtained potentials versus pH implies the existence of protonation processes that results in p*K* values for the oxidised and reduced states, presented in Table 2.

For processes I and II, assigned to Fe_B and heme b_3, the pH dependence is probably due to the protonable histidine residues that present pK_a range of 5.9–7.0. A conserved glutamate in the vicinity of Fe_B was already pointed as responsible for the second p*K* value, since it was proven that when buried in proteins these amino acids can present p*K* values of 8.5–8.8 [25,47,48]. The values found agree with previous work where the heme b_3 dependence on the pH was studied resulting

Table 2
P. nautica NOR pK_{ox} and pK_{red} for the different iron metal centres.

Metal centre	pK_{ox}[a]	pK_{red}[a]
Heme *c*	4.1	5.1
	7.2	8.2
Heme *b*	3.9	5.2
	7.1	8.4
Heme b_3	3.5	3.9
	5.3	6.3
	7.9	9.1
Fe_B	4.7	5.4
	8.6	9.7

[a] The determined error for all p*K*s is lower than 3.5%.

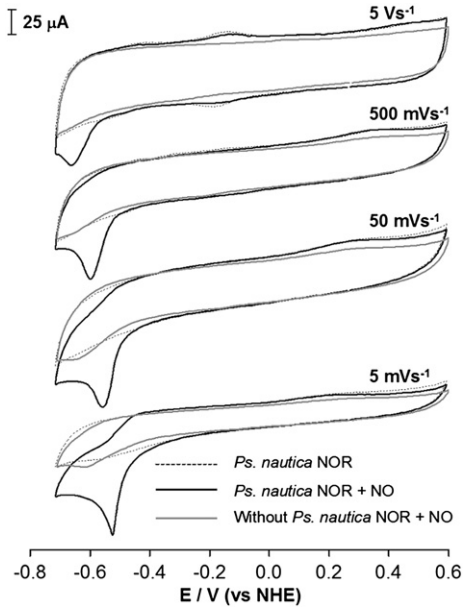

Fig. 4. Cyclic voltammograms of the immobilised NOR response in turnover conditions at different scan rates and control assays on bare electrode.

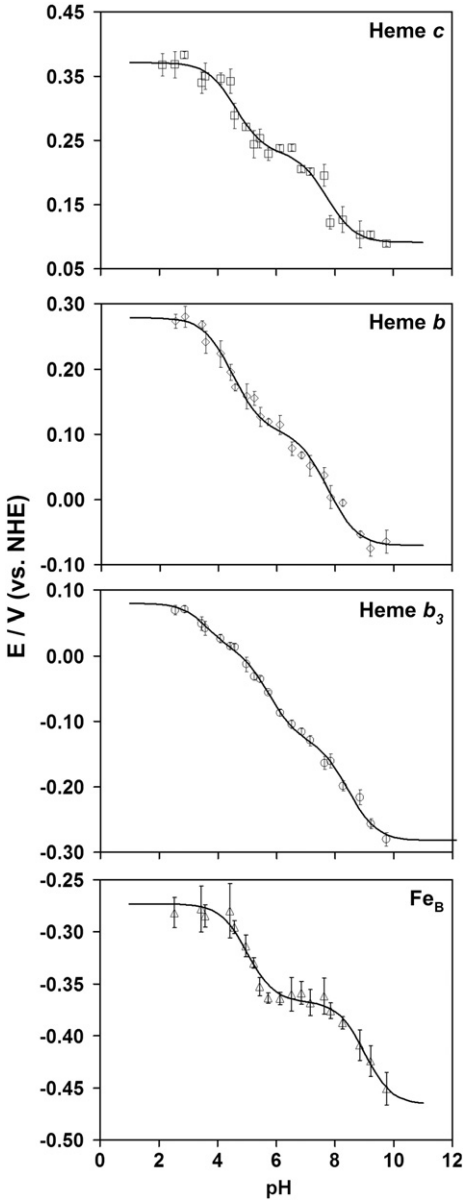

Fig. 5. Representation of the pH dependence of the *P. nautica* NOR midpoint redox potentials.

in four p*K* values for the oxidised and reduced states, namely, $pK_{ox1} = 5.0$, $pK_{red1} = 5.9$, $pK_{ox2} = 7.3$ and $pK_{red2} = 8.6$ [25].

The pH dependence of processes III and IV ascribed to the more positive potentials heme *b* and *c* centres shows similar behaviour. In both cases, the lower p*K* values determined can be attributed to the ionisation of the propionic side chains in the porphyrin ring. Usually these carboxyl groups show a pK_a close to 6, increasing when buried inside a protein or hydrophobic core, and much lower when exposed to the solvent or surrounded by a strong H-bond network [49]. A closer observation of the *P. aeruginosa* crystal structure shows that the low-spin heme *c* has high solvent exposure, and the propionic carboxyl groups are in close vicinity of three Arg residues (Arg 84, 85 and 109, *P. aeruginosa* numbering), which are conserved in the characterized cNOR from *Pseudomonas* species. In parallel, although heme *b* may have a lower solvent exposure, it is possible to find on its vicinity the conserved Arg 57 and Tyr 41 (*P. aeruginosa* numbering), facing the aliphatic side chains, which may form a strong H-bonding to the carboxyl groups [36]. The remaining p*K* values from hemes *c* and *b*, namely the values around 7 and 8 (see Table 2), can be assigned to the axial His residues present in both centres.

4. Concluding remarks

Direct electron transfer of NOR was attained in agreement with previous published work, resulting in the determination of the redox potentials of the four proteins' metallic centres. The binuclear iron centre presents the lowest redox potential, and discrimination between the heme b_3 and Fe_B redox processes was attained. The catalytic heme b_3 redox couple was observed close to −160 mV and a new process assigned to the non-heme Fe_B was observed at considerable lower potential values (approx. −370 mV), probably resulting from conformational changes required in the course of the NO catalytic cycle. This low potential is in agreement with a four electron reduced active state. Two other redox processes found at more positive potentials, approximately 40 and 200 mV, were associated to hemes *b* and *c*, respectively. From the number of electrons estimated it seems that all the redox processes correspond to a one-electron transfer. The four redox processes observed present pH dependence and the correspondent p*K* values were determined. The catalytic activity towards O_2 and NO was once again demonstrated by direct electrochemistry. From the experiments performed under turnover conditions, new data suggesting a *cis*-Fe_B mechanism was attained. The binding of ligands is expected to influence a metallic centre redox potential, as discussed earlier, and some authors have observed a significant shift in heme b_3 potential upon the binding of CO [27]. In our cyclic voltammetry assays, performed in the presence of NO, and in a potential window where the catalytic current of NO reduction is observed, if a NO molecule binds to heme b_3 a shift in its formal potential should be noticed, when comparing to assays in the absence of NO. Our data show that no potential shift is verified in these experimental conditions, which is in agreement with the *cis*-Fe_B model of NOR catalytic mechanism, suggesting that both NO molecules bind to Fe_B. Although there are many reports supporting both mechanisms and, in particular, the *trans* model, this new result seems to point to the *cis*-Fe_B, showing that the NOR catalytic mechanism is still under discussion.

Supplementary data to this article can be found online at http://dx.doi.org/10.1016/j.bbabio.2012.10.018.

Acknowledgements

The authors acknowledge the financial support of Fundação para a Ciência e Tecnologia (FCT/MCTES), grants PDTC/QUI/64638/2006, PDTC/QUI-BIQ/116481/2010 and SFRH/BD/39009/2007. REQUIMTE is funded by grant PEst-C/EQB/LA0006/2011 from FCT/MCTES.

References

[1] P. Tavares, A.S. Pereira, J.J. Moura, I. Moura, Metalloenzymes of the denitrification pathway, J. Inorg. Biochem. 100 (2006) 2087–2100.
[2] J. Reimann, U. Flock, H. Lepp, A. Honigmann, P. Adelroth, A pathway for protons in nitric oxide reductase from *Paracoccus denitrificans*, Biochim. Biophys. Acta 1767 (2007) 362–373.
[3] W.G. Zumft, Nitric oxide reductases of prokaryotes with emphasis on the respiratory, heme-copper oxidase type, J. Inorg. Biochem. 99 (2005) 194–215.
[4] S.J. Field, F.H. Thorndycroft, A.D. Matorin, D.J. Richardson, N.J. Watmough, The respiratory nitric oxide reductase (NorBC) from *Paracoccus denitrificans*, Methods Enzymol. 437 (2008) 79–101.
[5] G.J. Carr, S.J. Ferguson, The nitric oxide reductase of *Paracoccus denitrificans*, Biochem. J. 269 (1990) 423–429.
[6] J. Hoglen, T.C. Hollocher, Purification and some characteristics of nitric oxide reductase-containing vesicles from *Paracoccus denitrificans*, J. Biol. Chem. 264 (1989) 7556–7563.
[7] T. Sakurai, S. Nakashima, K. Kataoka, D. Seo, N. Sakurai, Diverse NO reduction by *Halomonas halodenitrificans* nitric oxide reductase, Biochem. Biophys. Res. Commun. 333 (2005) 483–487.
[8] T. Sakurai, N. Sakurai, H. Matsumoto, S. Hirota, O. Yamauchi, Roles of four iron centers in *Paracoccus halodenitrificans* nitric oxide reductase, Biochem. Biophys. Res. Commun. 251 (1998) 248–251.

[9] C.G. Timoteo, A.S. Pereira, C.E. Martins, S.G. Naik, A.G. Duarte, J.J. Moura, P. Tavares, B.H. Huynh, I. Moura, Low-spin heme b3 in the catalytic center of nitric oxide reductase from *Pseudomonas nautica*, Biochemistry 50 (2011) 4251–4262.
[10] D.H. Kastrau, B. Heiss, P.M. Kroneck, W.G. Zumft, Nitric oxide reductase from *Pseudomonas stutzeri*, a novel cytochrome bc complex. Phospholipid requirement, electron paramagnetic resonance and redox properties, Eur. J. Biochem. 222 (1994) 293–303.
[11] B. Heiss, K. Frunzke, W.G. Zumft, Formation of the N – N bond from nitric oxide by a membrane-bound cytochrome bc complex of nitrate-respiring (denitrifying) *Pseudomonas stutzeri*, J. Bacteriol. 171 (1989) 3288–3297.
[12] H. Kumita, K. Matsuura, T. Hino, S. Takahashi, H. Hori, Y. Fukumori, I. Morishima, Y. Shiro, NO reduction by nitric-oxide reductase from denitrifying bacterium *Pseudomonas aeruginosa*: characterization of reaction intermediates that appear in the single turnover cycle, J. Biol. Chem. 279 (2004) 55247–55254.
[13] J. Hendriks, A. Warne, U. Gohlke, T. Haltia, C. Ludovici, M. Lubben, M. Saraste, The active site of the bacterial nitric oxide reductase is a dinuclear iron center, Biochemistry 37 (1998) 13102–13109.
[14] T. Hino, Y. Matsumoto, S. Nagano, H. Sugimoto, Y. Fukumori, T. Murata, S. Iwata, Y. Shiro, Structural basis of biological N2O generation by bacterial nitric oxide reductase, Science (New York, N.Y.) 330 (2010) 1666–1670.
[15] P. Girsch, S. de Vries, Purification and initial kinetic and spectroscopic characterization of NO reductase from *Paracoccus denitrificans*, Biochim. Biophys. Acta 1318 (1997) 202–216.
[16] P. Moenne-Loccoz, S. de Vries, Structural characterization of the catalytic high-spin heme b of nitric oxide reductase: a resonance Raman study, J. Am. Chem. Soc. 120 (1998) 5147–5152.
[17] K.L. Gronberg, N.J. Watmough, A.J. Thomson, D.J. Richardson, S.J. Field, Redox-dependent open and closed forms of the active site of the bacterial respiratory nitric-oxide reductase revealed by cyanide binding studies, J. Biol. Chem. 279 (2004) 17120–17125.
[18] R.W. Ye, B.A. Averill, J.M. Tiedje, Denitrification: production and consumption of nitric oxide, Appl. Environ. Microbiol. 60 (1994) 1053–1058.
[19] T. Berto, A.L. Speelman, S. Zheng, N. Lehnert, Mono- and dinuclear non-heme iron-nitrosyl complexes: models for key intermediates in bacterial nitric oxide reductases, Coord. Chem. Rev. (2012), http://dx.doi.org/10.1016/j.ccr.2012.05.007.
[20] N.J. Watmough, M.R. Cheesman, C.S. Butler, R.H. Little, C. Greenwood, A.J. Thomson, The dinuclear center of cytochrome bo(3) from *Escherichia coli*, J. Bioenerg. Biomembr. 30 (1998) 55–62.
[21] L.M. Blomberg, M.R. Blomberg, P.E. Siegbahn, A theoretical study on nitric oxide reductase activity in a ba(3)-type heme-copper oxidase, Biochim. Biophys. Acta 1757 (2006) 31–46.
[22] P. Moenne-Loccoz, Spectroscopic characterization of heme iron-nitrosyl species and their role in NO reductase mechanisms in diiron proteins, Nat. Prod. Rep. 24 (2007) 610–620.
[23] N.J. Watmough, S.J. Field, R.J. Hughes, D.J. Richardson, The bacterial respiratory nitric oxide reductase, Biochem. Soc. Trans. 37 (2009) 392–399.
[24] K.L. Gronberg, M.D. Roldan, L. Prior, G. Butland, M.R. Cheesman, D.J. Richardson, S. Spiro, A.J. Thomson, N.J. Watmough, A low-redox potential heme in the dinuclear center of bacterial nitric oxide reductase: implications for the evolution of energy-conserving heme-copper oxidases, Biochemistry 38 (1999) 13780–13786.
[25] C.M. Cordas, A.S. Pereira, C.E. Martins, C.G. Timoteo, I. Moura, J.J. Moura, P. Tavares, Nitric oxide reductase: direct electrochemistry and electrocatalytic activity, ChemBioChem 7 (2006) 1878–1881.
[26] N. Yeung, Y.W. Lin, Y.G. Gao, X. Zhao, B.S. Russell, L. Lei, K.D. Miner, H. Robinson, Y. Lu, Rational design of a structural and functional nitric oxide reductase, Nature 462 (2009) 1079–1082.
[27] S.J. Field, M.D. Roldan, S.J. Marritt, J.N. Butt, D.J. Richardson, N.J. Watmough, Electron transfer to the active site of the bacterial nitric oxide reductase is controlled by ligand binding to heme b(3), Biochim. Biophys. Acta 1807 (2011) 451–457.
[28] E. Laviron, General expression of the linear potential sweep voltammogram in the case of diffusionless electrochemical systems, J. Electroanal. Chem. 101 (1979) 19–28.
[29] In: P.N. Bartlett (Ed.), Bioelectrochemistry—Fundamentals, Experimental Techniques and Applications, John Wiley & Sons, West Sussex, 2008.
[30] D. Sarauli, J. Tanne, D. Schafer, I.W. Schubart, F. Lisdat, Multilayer electrodes: fully electroactive cyt c on gold as a part of a DNA/protein architecture, Electrochem. Commun. 11 (2009) 2288–2291.
[31] F.A. Armstrong, R. Camba, H.A. Heering, J. Hirst, L.J.C. Jeuken, A.K. Jones, C. Leger, J.P. McEvoy, Fast voltammetric studies of the kinetics and energetics of coupled electron-transfer reactions in proteins, Faraday Discuss. 116 (2000) 191–203.
[32] D. Nkosi, J. Pillay, K.I. Ozoemena, K. Nouneh, M. Oyama, Heterogeneous electron transfer kinetics and electrocatalytic behaviour of mixed self-assembled ferrocenes and SWCNT layers, Phys. Chem. Chem. Phys. 12 (2010) 604–613.
[33] G.K. Rowe, M.T. Carter, J.N. Richardson, R.W. Murray, Consequences of kinetic dispersion on the electrochemistry of an adsorbed redox-active monolayer, Langmuir 11 (1995) 1797–1806.
[34] P. Lachmann, Y. Huang, J. Reimann, U. Flock, P. Adelroth, Substrate control of internal electron transfer in bacterial nitric-oxide reductase, J. Biol. Chem. 285 (2010) 25531–25537.
[35] K. Conrath, A.S. Pereira, C.E. Martins, C.G. Timoteo, P. Tavares, S. Spinelli, J. Kinne, C. Flaudrops, C. Cambillau, S. Muyldermans, I. Moura, J.J. Moura, M. Tegoni, A. Desmyter, Camelid nanobodies raised against an integral membrane enzyme, nitric oxide reductase, Protein Sci. 18 (2009) 619–628.
[36] T. Hino, Y. Matsumoto, S. Nagano, H. Sugimoto, Y. Fukumori, T. Murata, S. Iwata, Y. Shiro, Structural basis of biological N2O generation by bacterial nitric oxide reductase, Science (New York, N.Y.) 330 (2010) 1666–1670.
[37] U. Flock, N.J. Watmough, P. Adelroth, Electron/proton coupling in bacterial nitric oxide reductase during reduction of oxygen, Biochemistry 44 (2005) 10711–10719.
[38] J.P. Collman, N.K. Devaraj, R.A. Decreau, Y. Yang, Y.L. Yan, W. Ebina, T.A. Eberspacher, C.E.D. Chidsey, A cytochrome c oxidase model catalyzes oxygen to water reduction under rate-limiting electron flux, Science (New York, N.Y.) 315 (2007) 1565–1568.
[39] S. Yoshikawa, K. Muramoto, K. Shinzawa-Itoh, M. Mochizuki, Structural studies on bovine heart cytochrome c oxidase, Biochim. Biophys. Acta 1817 (2012) 579–589.
[40] M.S. Ram, L.M. Jones, H.J. Ward, Y.H. Wong, C.S. Johnson, P. Subramanian, J.T. Hupp, Ligand tuning effects upon the multielectron reduction and single-electron oxidation of (bi)pyridyl complexes of cis-dioxorhenium(V) and trans-dioxorhenium(V)—redox thermodynamics, preliminary electrochemical kinetics, and charge-transfer absorption-spectroscopy, Inorg. Chem. 30 (1991) 2928–2938.
[41] D. Faure, D. Lexa, J.M. Saveant, Electrochemistry of vitamin-B12.8. Thermodynamic and kinetic trans-effects in B12r–B12s oxido-reduction, J. Electroanal. Chem. 140 (1982) 285–295.
[42] H. Arii, Y. Funahashi, T. Ozawa, K. Jitsukawa, H. Masuda, Diiron(II) complexes showing a reversible oxygenation induced by a proton transfer mediated with a water molecule. Biological implication of a water molecule in hemerythrin function, J. Organomet. Chem. 692 (2007) 343–355.
[43] C. Belle, C. Beguin, I. Gautier-Luneau, S. Hamman, C. Philouze, J.L. Pierre, F. Thomas, S. Torelli, E. Saint-Aman, M. Bonin, Dicopper(II) complexes of H-BPMP-type ligands: pH-induced changes of redox, spectroscopic ((19)F NMR studies of fluorinated complexes), structural properties, and catecholase activities, Inorg. Chem. 41 (2002) 479–491.
[44] T.C. Berto, M.B. Hoffman, Y. Murata, K.B. Landenberger, E.E. Alp, J. Zhao, N. Lehnert, Structural and electronic characterization of non-heme Fe(II)-nitrosyls as biomimetic models of the FeB center of bacterial nitric oxide reductase (NorBC), J. Am. Chem. Soc. 133 (2011) 16714–16717.
[45] S.J. Elliott, A.E. McElhaney, C.J. Feng, J.H. Enemark, F.A. Armstrong, A voltammetric study of interdomain electron transfer within sulfite oxidase, J. Am. Chem. Soc. 124 (2002) 11612–11613.
[46] L.A. DeLouise, P.M. Kou, B.L. Miller, Cross-correlation of optical microcavity biosensor response with immobilized enzyme activity. Insights into biosensor sensitivity, Anal. Chem. 77 (2005) 3222–3230.
[47] J.J. Dwyer, A.G. Gittis, D.A. Karp, E.E. Lattman, D.S. Spencer, W.E. Stites, E.B. Garcia-Moreno, High apparent dielectric constants in the interior of a protein reflect water penetration, Biophys. J. 79 (2000) 1610–1620.
[48] C.A. Fitch, D.A. Karp, K.K. Lee, W.E. Stites, E.E. Lattman, E.B. Garcia-Moreno, Experimental pK(a) values of buried residues: analysis with continuum methods and role of water penetration, Biophys. J. 82 (2002) 3289–3304.
[49] G.R. Moore, G.W. Pettigrew, Cytochromes c Evolutionary, Structural and Physicochemical Aspects, Springer-Verlag, 1990.